Neurosci. Bull. October, 2019, 35(5):791–801
https://doi.org/10.1007/s12264-019-00372-x

www.neurosci.cn
www.springer.com/12264

ORIGINAL ARTICLE

Decreased miR-325-5p Contributes to Visceral Hypersensitivity Through Post-transcriptional Upregulation of CCL2 in Rat Dorsal Root Ganglia

Rui Wu[1,2] · Ping-An Zhang[1,2] · Xuelian Liu[2] · Yuan Zhou[2] · Meijie Xu[1] · Xinghong Jiang[2] · Jun Yan[3] · Guang-Yin Xu[1,2]

Received: 6 September 2018 / Accepted: 16 January 2019 / Published online: 12 April 2019

Abstract Chronic visceral hypersensitivity is an important type of chronic pain with unknown etiology and pathophysiology. Recent studies have shown that epigenetic regulation plays an important role in the development of chronic pain conditions. However, the role of miRNA-325-5p in chronic visceral pain remains unknown. The present study was designed to determine the roles and mechanism of miRNA-325-5p in a rat model of chronic visceral pain. This model was induced by neonatal colonic inflammation (NCI). In adulthood, NCI led to a significant reduction in the expression of miRNA-325-5p in colon-related dorsal root ganglia (DRGs), starting to decrease at the age of 4 weeks and being maintained to 8 weeks. Intrathecal administration of miRNA-325-5p agomir significantly enhanced the colorectal distention (CRD) threshold in a time-dependent manner. NCI also markedly increased the expression of CCL2 (C-C motif chemokine ligand 2) in colon-related DRGs at the mRNA and protein levels relative to age-matched control rats. The expression of CXCL12, IL33, SFRS7, and LGI1 was not significantly altered in NCI rats. CCL2 was co-expressed in NeuN-positive DRG neurons but not in glutamine synthetase-positive glial cells. Furthermore, CCL2 was mainly expressed in isolectin B4-binding- and calcitonin gene-related peptide-positive DRG neurons but in few NF-200-positive cells. More importantly, CCL2 was expressed in miR-325-5p-positive DRG neurons. Intrathecal injection of miRNA-325-5p agomir remarkably reduced the upregulation of CCL2 in NCI rats. Administration of Bindarit, an inhibitor of CCL2, markedly raised the CRD threshold in NCI rats in a dose- and time-dependent manner. These data suggest that NCI suppresses miRNA-325-5p expression and enhances CCL2 expression, thus contributing to visceral hypersensitivity in adult rats.

Keywords Visceral pain · Dorsal root ganglia · miRNA-325-5p · CCL2 · Epigenetic regulation

Introduction

MicroRNAs (miRs), small non-coding RNA molecules, contain 18–25 nucleotides [1]. They function in RNA-silencing and the post-transcriptional regulation of gene expression [2, 3]. It has been reported that miRs target different ion channels and receptors to modulate various physiological functions such as neurotransmission, immune reactions, inflammation, neurodegeneration, and nociception [4–6]. The dysregulation of miRs has been associated with many diseases such as cancer and obesity, as well as diseases of the gastrointestinal and nervous systems [1, 7, 8]. In recent years, many studies have delineated the post-transcriptional regulatory roles of miRs under chronic visceral pain conditions [5]. It has been reported that dysregulation of miR-146a-5p, miR-29a, and miR-199

Rui Wu and Ping-An Zhang have contributed equally to this work.

Electronic supplementary material The online version of this article (https://doi.org/10.1007/s12264-019-00372-x) contains supplementary material, which is available to authorized users.

✉ Guang-Yin Xu
guangyinxu@suda.edu.cn

[1] Center for Translational Medicine, Affiliated Zhangjiagang Hospital of Soochow University, Zhangjiagang 215600, China

[2] Department of Physiology and Neurobiology, Institute of Neuroscience, Soochow University, Suzhou 215123, China

[3] The Second Affiliated of Hospital Soochow University, Suzhou 215004, China

are closely associated with functional gastrointestinal disorders such as functional dyspepsia (FD) and irritable bowel syndrome (IBS) [5, 9]. miR-325 has been suggested to be associated with the risk of FD [10]. However, whether miR-325-5p is involved in IBS remains unclear.

One of the targets of miR-325-5p predicted by bioinformatics is C-C motif chemokine ligand 2 (CCL2), a small cytokine that belongs to the CC chemokine family [11]. CCL2 functions through its receptors CCR2 and CCR4, which are seven-transmembrane-domain G-protein-coupled receptors with a serine/threonine-rich intracellular C-terminal domain and an acidic N-terminal extracellular domain. An increasing body of evidence has demonstrated that CCL2 and its receptors are involved in inflammatory and neurodegenerative diseases including inflammatory pain and neuropathic pain [11–13]. However, whether CCL2 is involved in visceral pain and how it is regulated remains largely unknown.

Therefore, we hypothesized that neonatal colonic inflammation (NCI) suppresses miR-325-5p expression and subsequently leads to an increase in CCL2 expression in DRGs, thus contributing to the visceral hypersensitivity of the rats in adulthood. In the present study, we used a previously-established visceral pain model induced by NCI. This model mimics the main pathophysiological features of IBS in human patients [14, 15]. We showed for the first time that NCI resulted in downregulation of miR-325-5p in the DRGs of adult rats with colonic visceral hypersensitivity. We also demonstrated that NCI significantly enhanced the expression of CCL2 in DRGs. Our results suggest that miR-325-5p/CCL2 signaling is crucial for visceral pain and represents a potential strategy for the treatment of chronic visceral hypersensitivity (CVH) in patients with functional gastrointestinal disorders such as IBS.

Materials and Methods

Animals

All animals in our experiments were male Sprague-Dawley rats, weighing 180 g–250 g, provided by the Animal Care and Use Committee of Soochow University (Suzhou, China). Rats were housed under controlled conditions (24 °C ± 2 °C lights on 06:00–18:00) and had free access to food and water. We cared for and handled all rats following the guidelines of the International Association for the Study of Pain.

Neonatal Colonic Inflammation and Measurement of Chronic Visceral Hyperalgesia

Chronic visceral pain was induced by NCI as described previously [14, 16]. In brief, when pups were 10 days old, they were given an infusion of 0.2 mL acetic acid (0.5%, diluted in normal saline) into the colon. Control pups were given the same volume of normal saline (NS). Experiments were carried out on these rats at 4 weeks–10 weeks of age. Colorectal distention (CRD) was used to induce pain behavior as described previously [14, 17]. Briefly, under mild sedation (inhalation anesthesia by isoflurane), a flexible latex balloon (6 cm) attached to Tygon tubing was inserted 8 cm into the descending colon and rectum *via* the anus and held in place by taping the tubing to the tail. Rats were placed in small Lucite cubicles and allowed to adapt for 30 min. To minimize possible insult from the repetitive distention of the colon, the CRD threshold was measured as the minimal distention pressure in mmHg to evoke an abdominal visceromotor response to a steady increase in distention pressure *via* a sphygmomanometer.

Drug Administration

In behavioral experiments, miR-325-5p and negative control (NC) agomir/antagomir (from GenePharma, Shanghai, China) were delivered by intrathecal injection as reported previously [18, 19]. Briefly, under isoflurane inhalation anesthesia, rats were placed in a prone position and the L5–6 interspinous space was the puncture point. The vertical distance between the puncture point and the highest point in the rat's back was > 3 cm. The left side of the hip joint is located in the L5–6 spinous process space. The left thumb and middle finger were placed on both sides of this space and spread outward. The needle of a microsyringe held in the right hand was inserted vertically and slowly into the gap. When a tail-flick occurred, an assistant compressed the jugular vein on one side. Cerebrospinal fluid was withdrawn from the syringe and then the injection was performed. A tail-flick often occurred during the injection, indicating successful intrathecal administration. Bindarit (T6413, TargetMol, Boston, MA) was dissolved in dimethylsulfoxide and diluted with NS. The CRD threshold was measured after drug microinjection and tested until the effect of the drug had disappeared. The drug doses were chosen according to previous reports [20]. CCL2 (250-10, Peprotech, Rocky Hill, USA) was dissolved in ddH_2O and diluted with NS to 10 ng/μL. The dose of CCL2 used was 10 μL per rat, as in previous reports [21].

Western Blotting

Western blotting experiments were carried out as in our previous report [19]. The membrane was either incubated with anti-CCL2 antibody (1:500, ab25124, Abcam, Cambridge, UK) or anti-GAPDH antibody (1:200, sc-25778, Santa Cruz, CA, USA). All membranes were analyzed using ImageJ software (BIO-RAD, CA, USA). The CCL2 protein ($\sim$ 25 KD) expression was normalized to GAPDH ($\sim$ 37 KD).

Real-Time Quantitative PCR (QPCR)

RNA was extracted from the DRGs of control and NCI rats with TRIzol (15596026, Ambion, Shanghai, China). The cDNA of miR-325-5p and U6 was synthesized from total RNA using a reverse transcription kit (Applied Biosystems, Thermo Fisher Scientific, New York, USA); other cDNA were synthesized from total RNA using a reverse transcription kit (AE301-03, Transgen Biotech, Beijing, China) following the supplier's instructions. Bulge-loop melting temperature miRNA Q-RT primer sets specific for miR-325-5p and U6 (as an internal control) were designed by RiboBio (Guangzhou, China). The sequences of the primers used for QPCR are listed in Table 1.

Immunofluorescence Study and Fluorescence *In Situ* Hybridization

First, rats were deeply anesthetized and transcardially perfused with NS followed by 4% paraformaldehyde (Sinopharm Chemical Reagent Co. Ltd, Shanghai, China). The T13–L2 DRGs were then removed and postfixed for 0.5 h in paraformaldehyde and dehydrated in 10%, 20%, and 30% sucrose (Sinopharm Chemical Reagent Co. Ltd) in succession until sinking. The DRGs were cut at 14 μm on a freezing microtome (Leica, Wetzlar, Germany). For immunofluorescence, the sections were washed three times for 5 min each with phosphate-buffered saline, and incubated with blocking solution for 1 h, with primary antibodies overnight at 4°C, and then with secondary antibody [Alexa Fluor 488 (1:500, A21206, Molecular Probes New York, USA) and 555 (1:100, A31570, Molecular Probes New York, USA)] for 2 h at room temperature (RT). The primary antibody was omitted in negative controls. The primary antibodies used in the immunohistochemistry experiments were anti-CCL2 (1:1000, ab25124, Abcam, Cambridge, UK), anti-NeuN (1:50, MAB377, Merck Millipore, Germany), anti-GS (1:200, Abcam, Cambridge, UK), anti-CGRP (1:200, ab81887, Abcam, Cambridge, UK), anti-NF-200 (1:200, ab134306, Abcam, Cambridge, UK), and anti-IB4 (1:500, L2895, Sigma, St. Louis, MO).

Fluorescence *in situ* hybridization (FISH) was performed with Enhanced Sensitive ISH Detection Kit I (POD, Boster MK1030, Wuhan, China). A locked nucleic acid probe with complementarities to miR-325-5p was labeled with 5′ and 3′-digoxigenin and synthesized by Exiqon (Woburn, MA, USA). The slides were pre-hybridized for 2 h–4 h at 37°C, and then 1 μg/μL of probe in 60 μL–100 μL of hybridization mixture was added to each slide and incubated overnight at 37°C. Slides were incubated with 3% H_2O_2 for 30 min at RT to block endogenous peroxidases before applying horseradish peroxidase-conjugated antibodies. After washing, slides were incubated in blocking buffer for 30 min at RT, then 100 μL–150 μL antibodies were added and the slides were incubated for 30 min at RT. The slides were imaged under a fluorescence microscope, and the images were trimmed with Carl.Zeiss.AxioVision (Jena, Germany).

Table 1 Primer sequences.

Primers	Sequences (5′ to 3′)
CCL2-F	CTGTAGCATCCACGTGCTGT
CCL2-R	AGTTCTCCAGCCGACTCATTG
CXCL12-F	TGCATCAGTGACGGTAAGCC
CXCL12-R	TGAAGGGCACAGTTTGGAGT
LGI1-F	TCCCAAGACCTGCCTTACCA
LGI1-R	TGCAAAGCCATCCCGCTTAT
SFRS7-F	CCGACGAAGAAGAAGCAGGT
SFRS7-R	CCTGGATCTTGATCTCGACCTT
IL33-F	TAGCAAGCATGAAGGGAGGC
IL33-R	TGCAGGAAAGGAAGACTCGT
GAPDH-F	TGGAGTCTACTGGCGTCTT
GAPDH-R	TGTCATATTTCTCGTGGTTCA

Quantification and Statistics

All data are shown as the mean ± SEM. Statistical tests were applied depending upon the number of groups being compared. Normality was first examined for all data. When only two means were involved, a two-tailed *t*-test with unequal variances was used. When more than two means were involved, one-way analysis of variance (ANOVA) or Friedman ANOVA was first carried out to obtain a global test of the null hypothesis. If the global *P* value for the test was < 0.05, *post hoc* comparisons between the different groups using Dunn's *post hoc* test were applied. The Mann-Whitney test was used when the value was not normal. A comparison was considered statistically significant when the *P* value was < 0.05.

Results

NCI Downregulated miR-325-5p Expression in Colon-Related DRGs

Our previous studies have shown that NCI induces significant chronic visceral hypersensitivity [14, 22], and this was further confirmed by the present study. The distention thresholds of NCI rats were markedly lower than in control (CON) rats at 6 weeks and 8 weeks of age ($P < 0.05$ and < 0.01 *versus* CON, Mann-Whitney test) but did not differ at 4 weeks and 10 weeks (Fig. 1F–I). The distention thresholds in NCI rats were 32.10 ± 0.85 (n = 10 rats), 25.78 ± 1.38 (n = 6), 25.29 ± 1.51 (n = 7), and 34 ± 0.62 mmHg (n = 6), and in CON rats were 32.79 ± 0.88 (n = 9), 35.78 ± 0.84 (n = 9), 33.43 ± 1.56 (n = 7), and 35.56 ± 0.47 mmHg (n = 6) at 4 weeks, 6 weeks, 8 weeks, and 10 weeks, respectively. To determine whether miR-325-5p is involved, we used QPCR to measure its expression in colon-related DRGs (T13–L2) from NCI and CON rats at 2 weeks, 4 weeks, 6 weeks, 8 weeks, and 10 weeks of age (Fig. 1A–E). The relative miRNA levels in NCI rats at 2 weeks, 4 weeks, 6 weeks, 8 weeks, and 10 weeks were 1.59 ± 0.15 (n = 4 rats), 0.43 ± 0.11 (n = 3), 0.16 ± 0.08 (n = 5), 0.07 ± 0.04 (n = 5), and 0.98 ± 0.10 (n = 4), and in CON rats were 1.00 ± 0.25 (n = 4), 1.00 ± 0.10 (n = 3), 1.00 ± 0.15 (n = 4), 1.00 ± 0.19 (n = 4), and 1.00 ± 0.14 (n = 4), respectively. Statistical analysis showed that the miR-325-5p level was significantly lower in NCI than in CON rats at 4 weeks, 6 weeks, and 8 weeks ($P < 0.05$ and < 0.01 *vs* CON, two-tailed two-samples t-test). Furthermore, correlation analysis showed that the changes in distention threshold and miR-325-5p level had significant positive correlations at 6 weeks, 8 weeks, and 10 weeks (r = 0.99, P = 0.02). The (X, Y) values of the three points were (0.07, 25.29), (0.16, 25.78), and (0.98, 34.00). The values of distention threshold at 6, weeks 8 weeks, and 10 weeks were 25.78, 25.29 and 34.00 mmHg, respectively. The miR-325-5p levels at the corresponding time points were 0.16, 0.07, and 0.98, respectively (Fig. 1J). In addition, the expression of miR-325-5p was assessed in the cervical (C1–7) and lumbar (L4–6) DRGs as well as in the T13–L2 spinal cord at 6 weeks (Fig. S1A–C). The relative mRNA levels in NCI rats (n = 4) were 0.99 ± 0.10, 0.67 ± 0.10 and 0.68 ± 0.13, and in CON rats were 1.00 ± 0.06 (n = 4), 1.00 ± 0.11 (n = 4), and 1.00 ± 0.22 (n = 3). There was no significant change in these tissues when compared with age-matched control rats ($P > 0.05$ *vs* CON, two-tailed two-sample t-test). To validate the specific involvement of miR-325-5p in the visceral hypersensitivity of NCI rats, we also assessed the expression of other microRNAs. The relative mRNA levels of miR-7b, miR-466, and miR-142 in NCI rats were 0.69 ± 0.18 (n = 4 rats), 1.29 ± 0.17 (n = 6), and 1.06 ± 0.14 (n = 3), and in CON rats were 1.00 ± 0.18, 1.00 ± 0.23, and

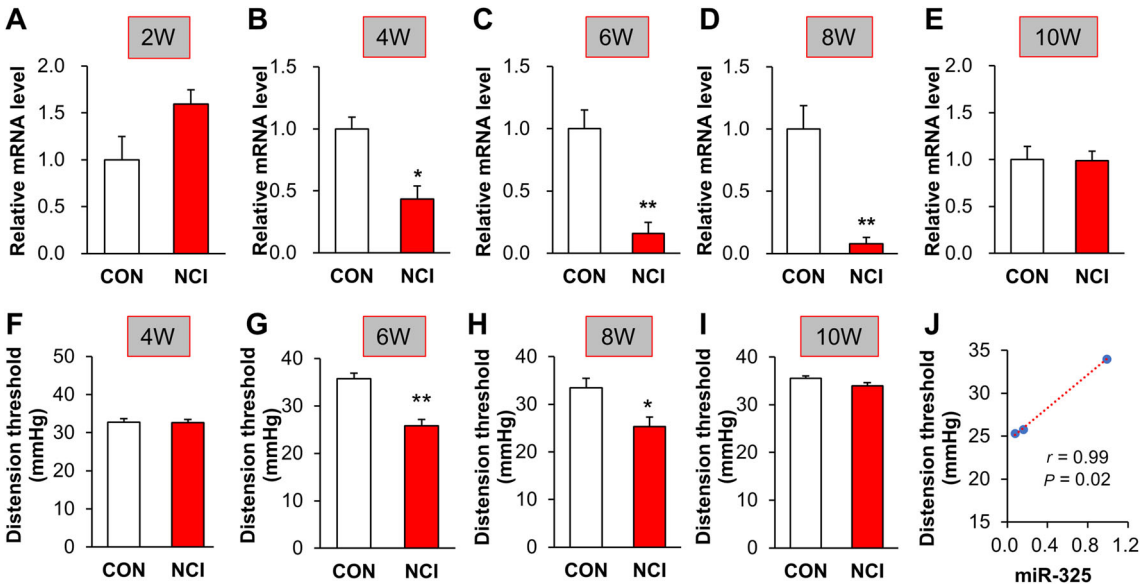

Fig. 1 NCI downregulated the expression of miR-325-5p in colon-related DRGs. **A** Quantification of QPCR assays showing that miR-325-5p expression was not changed in the colon-related T13–L2 DRGs of NCI rats at 2 weeks of age when compared with age-matched CON rats. **B–D** MiR-325-5p expression was significantly lower in the T13–L2 DRGs of NCI rats at 4 weeks, 6 weeks, and 8 weeks than in age-matched CON rats. **E** MiR-325-5p expression in T13–L2 DRGs did not differ between NCI and CON rats at 10 weeks. **F**, **I** The distension thresholds of NCI and CON rats did not differ at 4 weeks (**F**) and 10 weeks (**I**). **G**, **H** The distension threshold of NCI rats was markedly lower at 6 weeks and 8 weeks than in CON rats. **J** Correlation analysis showing a positive correlation between the CRD thresholds and miR-325 levels in NCI rats at 6 weeks, 8 weeks, and 10 weeks (r = 0.99, P = 0.02).

1.00 ± 0.11 (n = 4/group), respectively. There were no significant differences in the miR-7b, miR-466 and miR-142 levels between NCI and CON rats ($P > 0.05$ *vs* CON, two-tailed two-samples t-test, Fig. S1D–F). These results suggested that NCI suppresses the expression of miR-325-5p in colon-related DRGs.

Overexpression of miR-325-5p Reversed Visceral Hypersensitivity

To confirm the role of miR-325-5p in visceral hypersensitivity, we determined whether miR-325-5p antagomir induces visceral hypersensitivity in control rats. The CRD thresholds were measured in CON rats at 0.5 h, 1 h, 2 h, 4 h, and 8 h after intrathecal injection of miR-325-5p antagomir (10 μL, 20 μmol/L) or the same volume of antagomir-NC(negative control) (20 μmol/L). The CRD thresholds in control rats (n = 8 rats) treated with miR-325-5p antagomir were 19.31 ± 0.42, 19.25 ± 0.50, 20.75 ± 0.23, 27.00 ± 0.77, and 28.43 ± 1.17 mmHg, and in those treated with antagomir-NC (n = 6 rats) were 29.16 ± 0.38, 28.41 ± 0.25, 28.92 ± 0.40, 28.66 ± 0.42, and 28.25 ± 0.42 mmHg, respectively. The visceral hypersensitivity in the miR-325-5p antagomir group was significantly lower than in the antagomir-NC group from 0.5 h to 2 h but not at 4 h and 8 h (Fig. 2A, $P < 0.001$ *vs* NC, two-way ANOVA). In addition, we determined whether intrathecal injection of miR-325-5p agomir attenuates the visceral hypersensitivity in NCI rats (Fig. 2A). We first assessed the acute effect of miR-325-5p agomir by measuring the distention threshold 30 min after intrathecal injection of 10 μL (20 μmol/L) miR-325-5p agomir or agomir-NC. The distension thresholds of NCI rats at 0.5 h, 1 h, 2 h, 4 h, and 8 h after injection of miR-325-5p agomir were 23.05 ± 0.73, 27.43 ± 0.55, 29.81 ± 0.35, 19.24 ± 0.64, and 18.76 ± 0.17 mmHg (n = 7 rats), and after injection of agomir-NC were 19.11 ± 0.44, 19.44 ± 0.47, 19.88 ± 0.36, 19.66 ± 0.33, and 19.22 ± 0.23 mmHg (n = 6 rats), respectively. The distension threshold of NCI rats was significantly higher in the miR-325-5p agomir group than in the agomir-NC group at 0.5 h, 1 h, and 2 h after injection (Fig. 2A, $P < 0.01$ and $P < 0.001$ *vs* NC, two-way ANOVA).

Then we examined the chronic effect of miR-325-5p agomir. The same dose of miR-325-5p agomir or agomir-NC was injected every other day for a week (4 injections in total). After administration, the time-course of CRD thresholds was determined again. The CRD thresholds of NCI rats (6 weeks old) treated with miR-325-5p agomir were 30.27 ± 0.68, 30.19 ± 0.66, 31.81 ± 0.48, 35.81 ± 1.06, 30.38 ± 0.35, 32.28 ± 0.64, 31.61 ± 0.35, 20 ± 0.60, and 19.33 ± 0.71 mmHg (n = 7 rats) for 2 h, 4 h, 8 h, and 12 h, and 1, 2, 3, 4, and 5 days, while those of NCI rats treated with agomir-NC were 20.16 ± 0.83, 21.00 ± 0.72, 20.00 ± 0.40, 20.41 ± 0.52, 19.91 ± 0.68, 19.58 ± 0.53, 19.08 ± 1.27, 19.25 ± 0.57, and 19.16 ± 0.99 mmHg (n = 8 rats), respectively. The CRD thresholds in the miR-325-5p agomir group were significantly higher from 2 h to 3 days (Fig. 2B, $P < 0.001$ *vs* NC, two-way ANOVA) but not at 4 and 5 days (Fig. 2B, $P > 0.05$ *vs* NC, two-way ANOVA). These results suggested that overexpression of miR-325-5p reverses NCI-induced visceral hypersensitivity.

NCI Promoted CCL2 Expression in Colon-Related DRGs

miRs play their roles by acting on their downstream targets. We identified targets of miR-325-5p using two bioinformatics prediction online software (targetscan.org

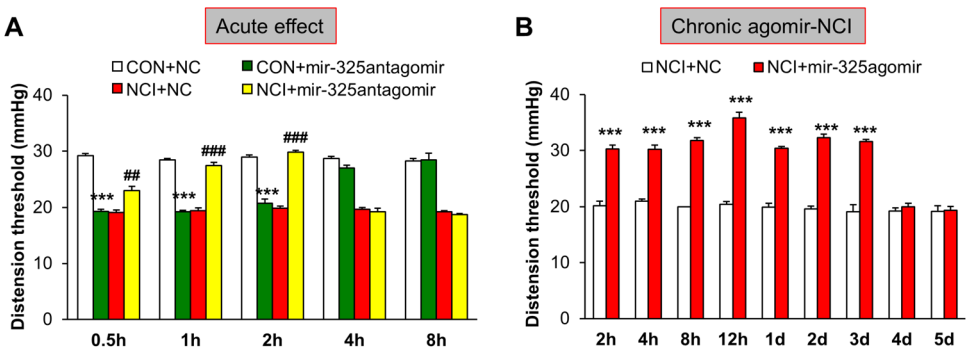

Fig. 2 Effects of miR-325-5p agomir and antagomir on visceral hypersensitivity. **A** CRD thresholds in control rats (CON, 6 weeks old) given miR-325-5p antagomir once (10 μL, 20 μmol/L) were significantly lower than in age-matched rats given the same volume of antagomir-NC (20 μmol/L) from 0.5 h to 2 h but not at 4 h and 8 h. The CRD thresholds in NCI rats given miR-325-5p agomir once (10 μL, 20 μmol/L) were significantly higher from 0.5 h to 2 h after injection than in age-matched NCI rats. This effect disappeared 4 h after injection. **B** NCI rats (6 weeks old) given miR-325-5p agomir (10 μL, 20 μmol/L) every other day for a week (4 injections in total) had higher CRD thresholds than age-matched NCI rats given the same dose of agomir-NC from 2 h to 3 days but not for 4 and 5 days.

and miRNA.org) and assessed the expression of CCL2 and CXCL12 that are related to CVH. QPCR analysis showed that the relative mRNA levels of CCL2 were 2.27 ± 0.38 (n = 5) in NCI rats and 1.00 ± 0.22 (n = 6) in CON rats and those of CXCL12 were 1.23 ± 0.10 (n = 4 rats) in NCI and 1.00 ± 0.32 (n = 3 rats) in CON. Interestingly, we found that NCI upregulated the expression of CCL2 (Fig. 3A, $P < 0.05$ *vs* CON, two-tailed two-sample t-test) but not CXCL12 (Fig. 3C, $P > 0.05$ *vs* CON, two-tailed two-sample t-test). In addition, we identified three high-score targets, IL33 (Interleukin 33), SFRS7 (Serine/arginine-rich splicing factor 7), and LGI1 (Leucine-rich glioma-inactivated protein 1), in the T13–L2 DRGs of 6-week-old rats (Fig. 3D–F). QPCR showed that the relative mRNA levels in NCI rats were 1.23 ± 0.15 (n = 3 rats), 0.75 ± 0.08 (n = 4), and 0.91 ± 0.02 (n = 4), and in CON rats were 1.00 ± 0.15 (n = 3), 1.00 ± 0.23 (n = 3), and 1.00 ± 0.05 (n = 3), respectively. There was no significant difference in the levels of these three molecules between the CON and NCI groups ($P > 0.05$ *vs* CON, two-tailed two-sample t-test). Furthermore, the protein level of CCL2 in T13–L2 DRGs at 6 weeks of age was assessed by western blotting (Fig. 3B). The relative densitometry of CCL2 in NCI rats was 0.40 ± 0.03 (n = 5) and 0.15 ± 0.04 for CON (n = 5), and the protein expression of CCL2 in T13–L2 DRGs was significantly higher ($P < 0.01$ *vs* CON, two-tailed two-sample t-test). This result was consistent with the mRNA levels of CCL2. These results suggested that NCI upregulates the expression of CCL2.

CCL2 Expression was Time-Dependent and Tissue-Specific

To further determine the time-course and specificity, the expression of CCL2 at 4 weeks, 8 weeks, and 10 weeks after NCI was then determined in T13–L2 DRGs by QPCR (Fig. 4A–C). The relative mRNA levels of CCL2 in NCI rats at 4 weeks, 8 weeks, and 10 weeks were 1.09 ± 0.20 (n = 5 rats), 2.29 ± 0.25 (n = 4), and 0.96 ± 0.21 (n = 3), while those in CON rats were 1.00 ± 0.17 (n = 5), 1.00 ± 0.18 (n = 4) and 1.00 ± 0.11 (n = 3), respectively, showing a significant increase at 8 weeks ($P < 0.01$ *vs* CON, two-tailed two-sample t-test) but not at 4 weeks and 10 weeks ($P > 0.05$ *vs* CON, two-tailed two-sample t-test). We also assessed the expression of CCL2 in the cervical DRGs (C1–7) of 6-week-old rats, and the QPCR results showed that the relative mRNA levels of CCL2 were 1.15 ± 0.17 (NCI, n = 3 rats) and 1.00 ± 0.14 (CON, n = 4); furthermore, these values in lumbar DRGs (L4–6) from age-matched rats were 0.68 ± 0.08 (NCI, n = 4) and 1.00 ± 0.21 (CON, n = 3). There was no significant change of CCL2 expression in C1–7 DRGs and L4–6 DRGs ($P > 0.05$ *vs* CON, two-tailed two-sample t-test) (Fig. 4D, E). More importantly, correlation analysis showed that the mRNA levels of CCL2 and the miRNA level of miR-325-5p were significantly negatively correlated at 6 weeks, 8 weeks, and 10 weeks (r = –0.997, P = 0.046, Fig. 4F). The values of the relative miR-325-5p levels at 6 weeks, 8 weeks, and 10 weeks were 0.16, 0.07, and 0.98, while those of of CCL2 were 2.27, 2.29, and 0.96, respectively. The (X, Y) values of the 3 points in Fig. 4F were (0.07, 2.29), (0.16, 2.27), and (0.98, 0.96).

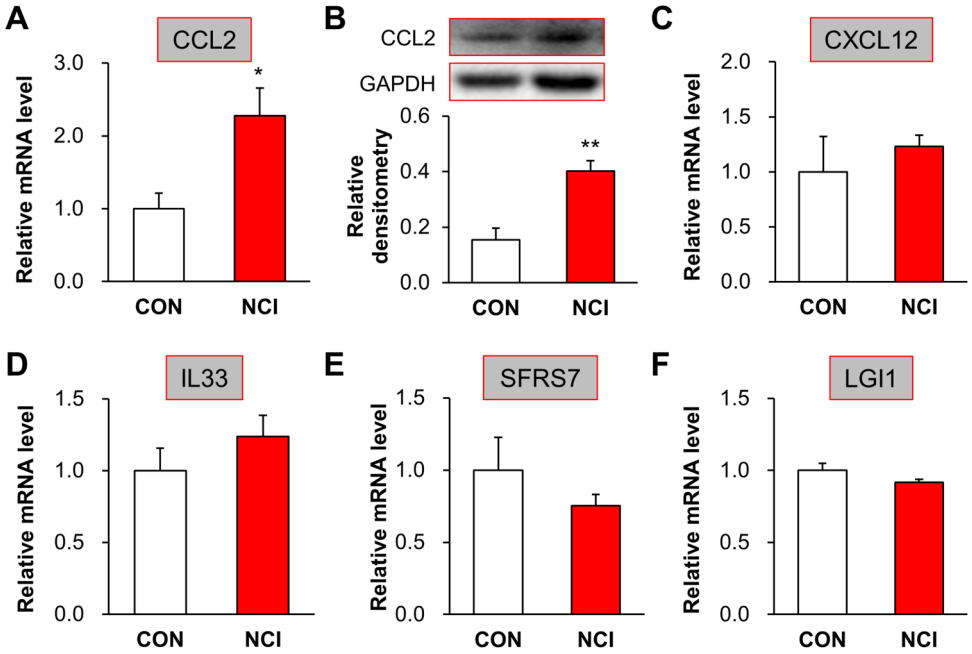

Fig. 3 Expression of CCL2, CXCL12, IL33, SFRS7, and LGI1 mRNA, and protein expression of CCL2. **A** Quantification of QPCR assays showing significant up-regulation of CCL2 mRNA expression in T13–L2 DRGs of 6-week-old NCI rats compared with age-matched CON rats. **B** Protein expression of CCL2 in T13–L2 DRGs was significantly higher than in CON rats at 6 weeks. **C–F** mRNA levels of CXCL12, IL33, SFRS7, and LGI1 in the T13–L2 DRGs of NCI rats did not differ from CON rats.

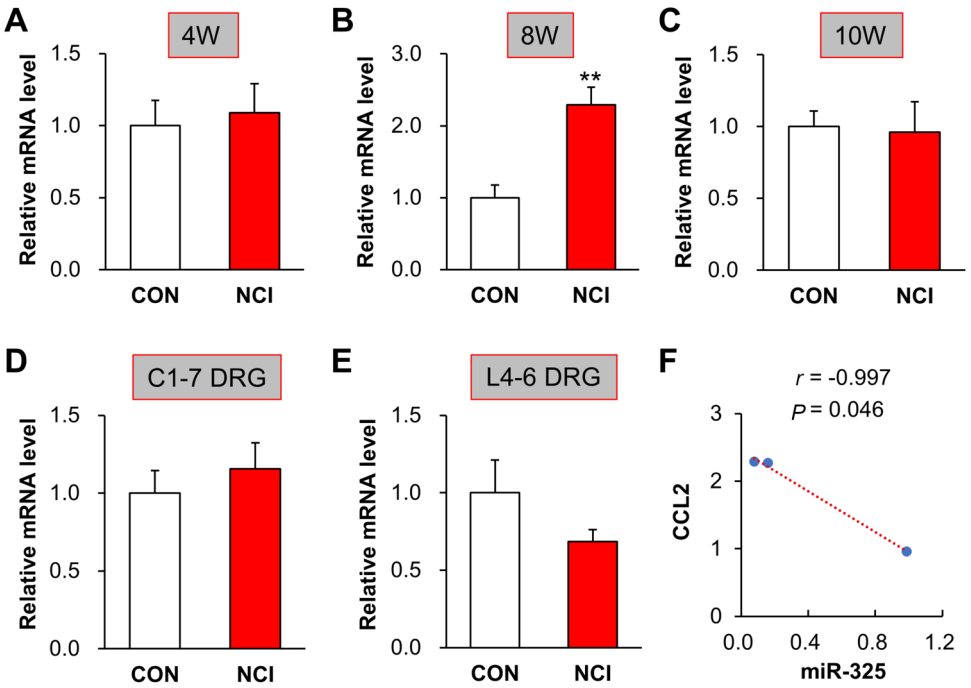

Fig. 4 CCL2 expression was time-dependent and tissue-specific. **A** QPCR data showing that the mRNA expression of CCL2 in T13–L2 from NCI rats did not differ from CON rats at 4 weeks of age. **B** QPCR analysis showing that the mRNA level of CCL2 was significantly higher in NCI rats than CON rats at 8 weeks of age. **C** QPCR analysis also showed no significant difference of CCL2 in T13–L2 DRGs between NCI and CON rats at 10 weeks of age. **D**, **E** NCI did not change the expression of CCL2 of cervical (C1–7) DRGs and lumbar (L4–6) DRGs at 6 weeks of age. **F** Significant negative correlation in the relative mRNA levels of CCL2 and miR-325 at 6 weeks, 8 weeks, and 10 weeks ($r = -0.997$, $P < 0.05$).

Location of CCL2 in Colon-Related DRGs

We then determined the location of CCL2 in DRGs using immunofluorescence. We co-labelled CCL2 with glutamine synthetase (GS) (a marker of satellite glial cells) or NeuN (a marker of neurons) to determine the localization of CCL2 in colon-related DRGs (Fig. 5A). The results showed that CCL2 was co-expressed in neurons but not

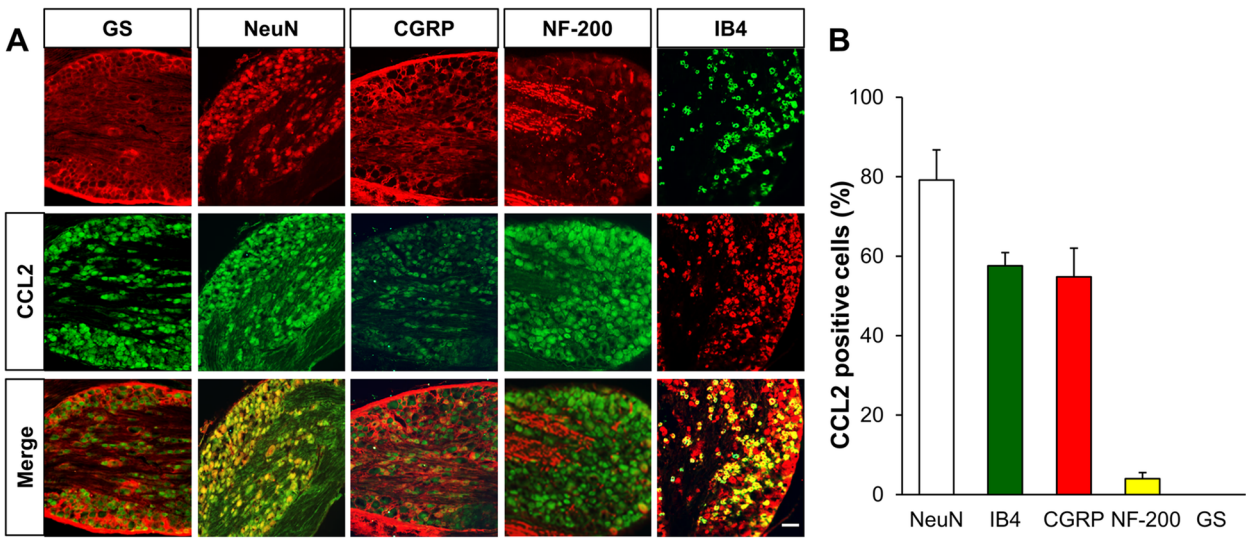

Fig. 5 Immunofluorescence analysis of CCL2 in colon-related DRGs. **A** CCL2-positive DRG cells (middle row) were co-labeled as neuron-positive (upper left second, red) but not with GS-positive cells (upper left first, red). CCL2 was co-expressed in IB4-positive (upper right first, green), CGRP-positive (upper middle, red) and NF-200-positive (upper right second, red) DRG neurons. Merges of CCL2 with GS, NeuN, CGRP, NF-200, and IB4 are shown in the lower row. Scale bar, 50 μm. **B** Quantification showing that CCL2 was mainly located in small and medium sensory neurons labeled with IB4 and CGRP but a few with NF-200.

satellite glial cells. Furthermore, we co-stained CCL2 with NF-200 (a marker of large neurons), isolectin B4 (IB4, a marker of non-peptidergic small and medium neurons), and calcitonin gene-related peptide (CGRP, a marker of small and medium peptidergic neurons) by immunofluorescence and showed that CCL2 was mainly located in small and medium sensory neurons labeled with IB4 and CGRP but in few with NF-200. Analysis showed that the percentage co-localization of CCL2 with NeuN, IB4, CGRP, NF-200. and GS was 79.17, 57.59, 54.8, 3.99, and 0% (n = 3), respectively (Fig. 5B).

Overexpression of miR-325-5p Reversed the Increase of CCL2 Expression at the Protein Level

A precondition for a reaction between miR-325-5p and CCL2 is that the two molecules are co-expressed in the same type of cell, so we used an RNA probe of miR-325-5p to perform FISH and determine whether the two molecules are co-localized in T13–L2 DRGs. As shown in Fig. 6A, miR-325-5p was co-expressed with CCL2 in the same neurons of colon-related DRGs; the percentage of miR-325-5p co-labeled with CCL2 and NeuN was 82.46% and 87.35% (n = 3) (Fig. 6B). To verify the hypothesis that down-regulation of miR-325-5p contributes to visceral hypersensitivity *via* up-regulation of CCL2 in DRGs, we first overexpressed miR-325-5p by intrathecal injection of its agomir, and 0.5 h later measured the protein expression of CCL2 in T13–L2 DRGs (Fig. 6C). The results showed no significant difference in CCL2 protein expression between NCI rats given miR-325-5p agomir and those given agomir-NC ($P > 0.05$, two-tailed two-sample t-test). Then, the expression of CCL2 in T13–L2 DRGs of NCI rats was assessed 12 h after delivery of miR-325-5p agomir or agomir-NC. Western blots showed that the relative densitometry of CCL2 in NCI rats treated with miR-325-5p agomir was 0.21 ± 0.06 (n = 4), and in those treated with agomir-NC was 0.42 ± 0.03 (n = 4). The CCL2 protein

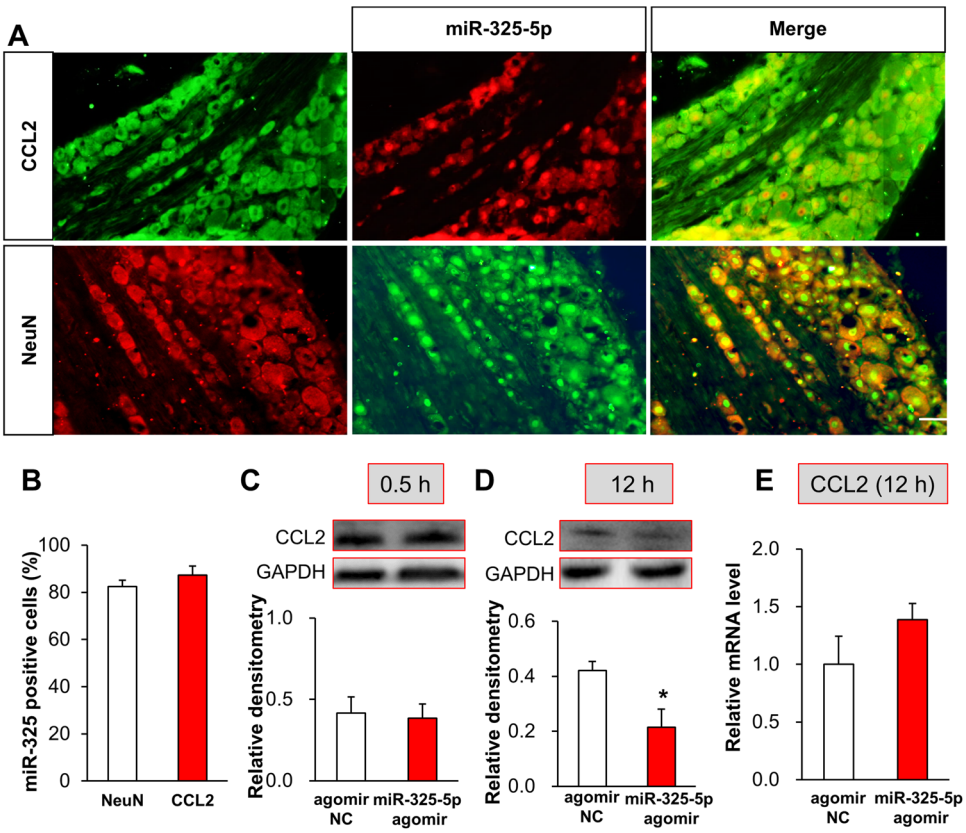

Fig. 6 Reactions of miR-325-5p and CCL2. **A** Fluorescence *in situ* hybridization for miR-325-5p and CCL2 showing CCL2-positive cells (green, upper left) and miR-325-5p-positive cells (red, upper middle) co-expressed in DRG neurons (upper right), and NeuN-positive cells (red, lower left) co-expressed with miR-325-5p (green, lower middle). Lower right merged miR-325-5p with NeuN. Scale bar, 50 μm. **B** Analysis showing that miR-325-5p was mainly co-expressed with CCL2 in colon-related DRG neurons. **C** Western blots and quantification of CCL2 expression in T13–L2 DRGs showing no significant difference between NCI 6-week-old rats given miR-325-5p agomir and those given agomir-NC at 0.5 h after injection. **D** Western blots and quantification of CCL2 in T13–L2 DRGs showing that NCI rats (6 weeks) given miR-325-5p agomir showed a significant decrease compared with age-matched NCI rats given agomir-NC at 12 h after injection. **E** CCL2 mRNA expression was not significantly altered 12 h after intrathecal injection of miR-325-5p agomir when compared with the agomir-NC group.

expression was significantly lower 12 h after intrathecal injection of miR-325-5p agomir than in the agomir-NC group (Fig. 6D, $P < 0.05$ *vs* NC, two-tailed two-sample *t*-test). In contrast, CCL2 mRNA expression was not significantly altered after intrathecal injection of miR-325-5p agomir when compared with the agomir-NC group (Fig. 6E, $P > 0.05$ *vs* NC, two-tailed two-sample *t*-test).

Inhibition of CCL2 Attenuates Visceral Hypersensitivity in NCI Rats

CCL2, also known as monocyte chemoattractant protein-1, is a chemokine. Recent studies have reported that it plays an important role in pain [11]. To confirm its role in CVH induced by NCI, we used Bindarit, a selective inhibitor of CCL2. Bindarit at 1, 10, and 100 μmol/L was administered. The baseline CRD thresholds of the 4 groups of NCI rats before drug administration were 18.91 ± 0.24 (NS, $n = 6$ rats), 19.91 ± 0.20 (1 μmol/L, $n = 6$), 17.78 ± 0.34 (10 μmol/L, $n = 7$), and 20.87 ± 0.33 mmHg (100 μmol/L, $n = 6$). After treatment with 1, 10, and 100 μmol/L Bindarit for 1 h and 2 h, the CRD thresholds were 20.33 ± 0.36 ($n = 6$) and 19.75 ± 0.36 ($n = 6$); 26.64 ± 1.29 ($n = 7$) and 27.21 ± 0.56 ($n = 6$); and 34.75 ± 1.22 ($n = 6$) and 37.58 ± 1.29 mmHg ($n = 6$), respectively. NS or 1 μmol/L Bindarit did not change the CRD thresholds of NCI rats ($P > 0.05$ *vs* baseline, two-way ANOVA), but 10 and 100 μmol/L Bindarit both induced a significant increase in CRD threshold at 1 h and 2 h (Fig. 7A, $P < 0.001$ *vs* baseline, two-way ANOVA). We next determined the time-course of the Bindarit effect at 10 μmol/L. Bindarit was injected once daily for 7 consecutive days. The CRD threshold before injection was 18.66 ± 0.56 mmHg ($n = 6$ rats) and after administration for 1, h 2 h, 4 h, 8 h, and 12 h, and 1, 2, and 3 days was 29.08 ± 0.32, 30.36 ± 0.54, 30.7 ± 1.21, 34.4 ± 2.07, 33.2 ± 1.45, 28.2 ± 1.19, 19.2 ± 1.07, and 19.48 ± 0.44 mmHg, respectively, showing a significant increase from 1 h and lasting for 1 day (Fig. 7B, $P < 0.001$ *vs* baseline, one-way ANOVA). To determine whether CCL2 induces CVH in 6-week-old naïve rats, their thresholds were measured after intrathecal delivery of CCL2 (100 ng per rat). The CRD threshold before injection was 30.69 ± 0.34 mmHg ($n = 8$ rats) and 0.5 h, 1 h, 2 h, 4 h, and 8 h after administration was 26.83 ± 0.46, 26.38 ± 0.63, 25.6 ± 0.69, 28.44 ± 0.50, and 31.09 ± 0.42 mmHg, respectively. These results showed that intrathecal CCL2 significantly reduced the CRD thresholds at 0.5 h, 1 h, 2 h, and 4 h (Fig. 7C, $P < 0.001$ *vs* baseline, two-way ANOVA), indicating that CCL2 is involved in the CVH induced by NCI.

Discussion

In the present study, we demonstrated for the first time that miR-325-5p is involved in the colonic CVH induced by NCI, a conclusion based on the following findings. The expression of miR-325-5p was significantly decreased in the colon-related DRGs of rats with visceral pain. The down-regulation of miR-325-5p in these DRGs appeared at 4 weeks, 6 weeks, and 8 weeks, which well matched the visceral pain responses of NCI rats. Importantly, up-regulation of miR-325-5p by intrathecal injection of miR-325-5p agomir markedly raised the CRD threshold of NCI rats. In contrast, inhibition of miR-325-5p by intrathecal

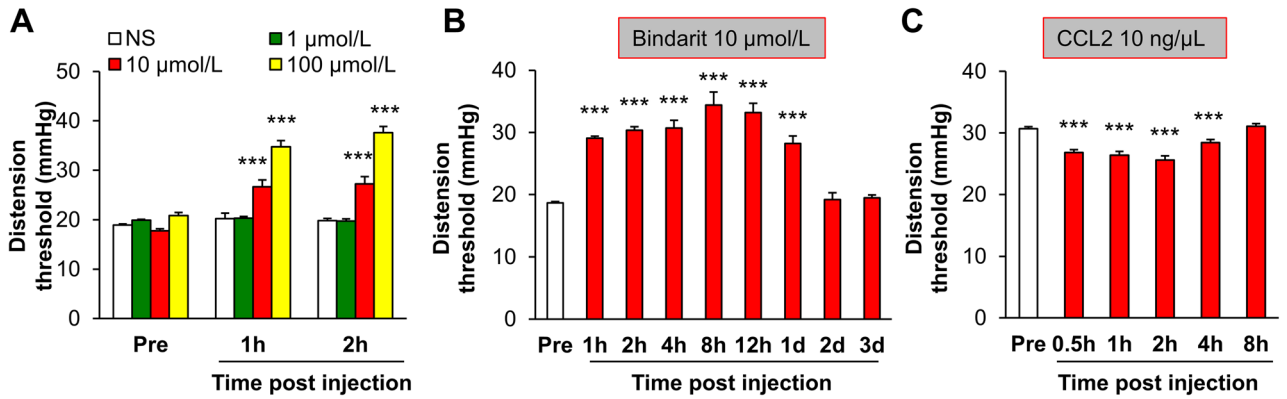

Fig. 7 Suppression of CVH by Bindarit. **A** Distension thresholds of NCI rats 1 h and 2 h after delivery of NS and 1, 10, and 100 μmol/L. Bindarit showed no difference between NCI rats given NS or 1 μmol/L Bindarit and baseline (Pre). The CRD thresholds for NCI rats given 10 and 100 μmol/L were significantly higher than baseline (Pre). **B** Time-dependent effect of 10 μmol/L Bindarit showed significant changes in the CRD thresholds of NCI rats from 1 h to 1 day relative to baseline (Pre). This effect disappeared after 1 day. **C** Intrathecal injection of CCL2 significantly reduced the CRD threshold of 6-week-old naïve rats at 0.5 h, 1 h, 2 h, and 4 h compared with baseline (Pre).

injection of miR-325-5p antagomir remarkably lowered the CRD threshold of healthy control rats. Therefore, we add new evidence to support an idea that microRNAs are critical in the development of the CVH associated with functional gastrointestinal disorders.

Researchers in the field of miR signaling have demonstrated that miR-325 plays an important role in cancer [23], functional dyspepsia [10], and hypoxic-ischemic brain injury [6]. However, whether miR-325 is involved in visceral pain responses was unclear. Here, we showed that miR-325-5p was down-regulated while the expression of three other miRNAs was not altered, indicating a role of miR-325-5p in chronic visceral pain. The expression of miR-325-5p was not changed in other tissues such as DRGs unrelated to the colon and in the dorsal spinal cord, indicating tissue-specific up-regulation of miR-325-5p expression. Although we cannot exclude roles of miR-7b, miR-466, and miR-142 in chronic visceral pain, our data suggest that down-regulation of miR-325-5p contributes to visceral pain since application of miR-325-5p agomir significantly reversed the CRD threshold of NCI rats.

Using a combination of bioinformatics resources with enrichment of annotations based on functional ontologies and a spatiotemporal expression dataset [24], we found that miR-325-5p could bind to the 3'UTR of CCL2 mRNA. MiR-325-5p has >100 targets. The reason we studied CCL2 was that it is involved in inflammatory pain, neuropathic pain, and visceral hypersensitivity [25, 26]. We demonstrated here that CCL2 in colon-related DRGs was involved in visceral pain in NCI rats. First of all, CCL2 was up-regulated at both the protein and mRNA levels in the colon-related DRGs of NCI rats at 6 weeks and 8 weeks, while the expression of other targets did not change. This is consistent with previous reports that CCL2 expression is enhanced under neuropathic pain conditions [11, 27]. Second, inhibition of CCL2 by Bindarit significantly increased the CRD threshold of NCI rats. Once upregulated, CCL2 may be released from the soma and subsequently activate CCR2 and CCR4, thus enhancing DRG neuronal excitability [28]. We also showed that the Bindarit effect lasted only for one day, but we do not know the exact reasons why this effect is so short. One possibility is that Bindarit is degraded rapidly *in vivo*, another might be that the upregulation of CCL2 is not the only mechanism involved in colonic hypersensitivity. When CCL2 is inhibited by Bindarit, other pathways may be activated. Besides, a brief inhibitory effect of this drug has been reported in many other models [29, 30]. In addition, CCL2 in DRG neurons can be transported to central terminals at the spinal cord level since it is present in the central terminals of primary afferents in the superficial dorsal horn [31, 32]. Once released from the central terminals, CCL2 activates its receptors on dorsal horn neurons, thus enhancing synaptic transmission in the dorsal horn. Thus, CCL2 might be a modulator to increase DRG neuronal excitability and spinal synaptic transmission that we have reported previously under NCI-induced visceral pain conditions [14, 22].

MicroRNAs are involved in the regulation of cellular life by targeting specific mRNAs to repress their translation or degrade them. It was therefore of interest to determine whether and how miR-325-5p modulates CCL2 expression. We showed using immunofluorescence and FISH that miR-325-5p was co-localized with CCL2 in DRG neurons, indicating the anatomical possibility that miR-325-5p regulates CCL2 expression. Then, application of miR-325-5p agomir clearly reversed the up-regulation of CCL2 in colon-related DRGs at the protein level but not at the mRNA level. These results seemed inconsistent but suggested that miR-325-5p regulates CCL2 expression through post-transcriptional machinery. One question that remains is the mechanism by which CCL2 mRNA is up-regulated under NCI-induced visceral pain conditions. Since application of miR-325-5p agomir did not reverse the up-regulation of CCL2 at the mRNA level, other mechanisms might be involved, and this warrants a further investigation. Beyond that, how miR-325 agomir has such a rapid effect on the CRD threshold remains unknown. Recently, Ji's group demonstrated that miR-711 induces inward currents and action potentials *via* transient receptor potential ankyrin 1 in mouse DRG neurons, which suggests that miRs can directly activate ion channels to affect excitability [33]. This might be one of the mechanisms underlying the rapid effects of miRs. In addition, how miR-325-5p is suppressed also needs further investigation. Nevertheless, our findings suggest that miR-325-5p negatively modulates CCL2 expression most likely through a post-transcriptional mechanism.

In summary, we demonstrated that miR-325-5p/CCL2 signaling is important in the development of visceral pain in NCI rats. The current findings of miR-325-5p dysfunction in colon-related DRGs point to the importance of future work investigating the role of miRs in understanding chronic visceral pain in patients with functional gastrointestinal disorders such as IBS.

Acknowledgements This work was supported by grants from the National Natural Science Foundation of China (81471137, 31730040, and 81771187) and from the Priority Academic Program Development of Jiangsu Higher Education Institutions of China.

Conflict of interest No conflicts of interest, financial or otherwise, are declared by the authors.

References

1. Wang Y, Yang Z, Le W. Tiny but mighty: promising roles of micrornas in the diagnosis and treatment of parkinson's disease. Neurosci Bull 2017, 33: 543–551.
2. Ambros V. The functions of animal micrornas. Nature 2004, 431: 350–355.
3. Bartel DP. Micrornas: Genomics, biogenesis, mechanism, and function. Cell 2004, 116: 281–297.
4. Zhang J, Banerjee B. Role of microrna in visceral pain. J Neurogastroenterol Motil 2015, 21: 159–171.
5. Zhou Q, Yang L, Larson S, Basra S, Merwat S, Tan A, *et al.* Decreased mir-199 augments visceral pain in patients with ibs through translational upregulation of trpv1. Gut 2016, 65: 797–805.
6. Yang Y, Sun B, Huang J, Xu L, Pan J, Fang C, *et al.* Up-regulation of mir-325-3p suppresses pineal aralkylamine n-acetyltransferase (aanat) after neonatal hypoxia-ischemia brain injury in rats. Brain Res 2017, 1668: 28–35.
7. Arshad AR, Sulaiman SA, Saperi AA, Jamal R, Mohamed Ibrahim N, Abdul Murad NA. Micrornas and target genes as biomarkers for the diagnosis of early onset of parkinson disease. Front Mol Neurosci 2017, 10: 352.
8. Zhou Q, Verne GN. Role of microrna in chronic visceral nociception. Pain 2013, 154: 9–10.
9. Lu Y, Cao DL, Jiang BC, Yang T, Gao YJ. Microrna-146a-5p attenuates neuropathic pain via suppressing traf6 signaling in the spinal cord. Brain Behav Immun 2015, 49: 119–129.
10. Arisawa T, Tahara T, Fukuyama T, Hayashi R, Matsunaga K, Hayashi N, *et al.* Genetic polymorphism of pri-microrna 325, targeting slc6a4 3'-utr, is closely associated with the risk of functional dyspepsia in japan. J Gastroenterol 2012, 47: 1091–1098.
11. Miotla Zarebska J, Chanalaris A, Driscoll C, Burleigh A, Miller RE, Malfait AM, *et al.* Ccl2 and ccr2 regulate pain-related behaviour and early gene expression in post-traumatic murine osteoarthritis but contribute little to chondropathy. Osteoarthritis Cartilage 2017, 25: 406–412.
12. Zheng Y, Qin L, Zacarias NV, de Vries H, Han GW, Gustavsson M, *et al.* Structure of cc chemokine receptor 2 with orthosteric and allosteric antagonists. Nature 2016, 540: 458–461.
13. Van Steenwinckel J, Auvynet C, Sapienza A, Reaux-Le Goazigo A, Combadiere C, Melik Parsadaniantz S. Stromal cell-derived ccl2 drives neuropathic pain states through myeloid cell infiltration in injured nerve. Brain Behav Immun 2015, 45: 198–210.
14. Xu GY, Shenoy M, Winston JH, Mittal S, Pasricha PJ. P2x receptor-mediated visceral hyperalgesia in a rat model of chronic visceral hypersensitivity. Gut 2008, 57: 1230–1237.
15. Zhu L, Zhao L, Qu R, Zhu HY, Wang Y, Jiang X, *et al.* Adrenergic stimulation sensitizes trpv1 through upregulation of cystathionine beta-synthetase in a rat model of visceral hypersensitivity. Sci Rep 2015, 5: 16109.
16. Yuan B, Tang WH, Lu LJ, Zhou Y, Zhu HY, Zhou YL, *et al.* Tlr4 upregulates cbs expression through nf-kappab activation in a rat model of irritable bowel syndrome with chronic visceral hypersensitivity. World J Gastroenterol 2015, 21: 8615–8628.
17. Du WJ, Hu S, Li X, Zhang PA, Jiang X, Yu SP, *et al.* Neonatal maternal deprivation followed by adult stress enhances adrenergic signaling to advance visceral hypersensitivity. Neurosci Bull 2019, 35: 4–14.
18. Kong X, Wei J, Wang D, Zhu X, Zhou Y, Wang S, *et al.* Upregulation of spinal voltage-dependent anion channel 1 contributes to bone cancer pain hypersensitivity in rats. Neurosci Bull 2017, 33: 711–721.
19. Dalgarno R, Leduc-Pessah H, Pilapil A, Kwok CH, Trang T. Intrathecal delivery of a palmitoylated peptide targeting y382-384 within the p2x7 receptor alleviates neuropathic pain. Mol Pain 2018, 14: 1744806918795793.
20. Su S, Shao J, Zhao Q, Ren X, Cai W, Li L, *et al.* Mir-30b attenuates neuropathic pain by regulating voltage-gated sodium channel nav1.3 in rats. Front Mol Neurosci 2017, 10: 126.
21. Hu JH, Zheng XY, Yang JP, Wang LN, Ji FH. Involvement of spinal monocyte chemoattractant protein-1 (mcp-1) in cancer-induced bone pain in rats. Neurosci Lett 2012, 517: 60–63.
22. Zhao L, Xiao Y, Weng RX, Liu X, Zhang PA, Hu CY, *et al.* Neonatal colonic inflammation increases spinal transmission and cystathionine beta-synthetase expression in spinal dorsal horn of rats with visceral hypersensitivity. Front Pharmacol 2017, 8: 696.
23. Li H, Huang W, Luo R. The microrna-325 inhibits hepatocellular carcinoma progression by targeting high mobility group box 1. Diagn Pathol 2015, 10: 117.
24. Abidin SZ, Leong JW, Mahmoudi M, Nordin N, Abdullah S, Cheah PS, *et al.* In silico prediction and validation of gfap as an mir-3099 target in mouse brain. Neurosci Bull 2017, 33: 373–382.
25. Distrutti E, Cipriani S, Mencarelli A, Renga B, Fiorucci S. Probiotics vsl#3 protect against development of visceral pain in murine model of irritable bowel syndrome. PLoS One 2013, 8: e63893.
26. Illias AM, Gist AC, Zhang H, Kosturakis AK, Dougherty PM. Chemokine ccl2 and its receptor ccr2 in the dorsal root ganglion contribute to oxaliplatin-induced mechanical hypersensitivity. Pain 2018, 159:1308-1316.
27. Tanaka T, Minami M, Nakagawa T, Satoh M. Enhanced production of monocyte chemoattractant protein-1 in the dorsal root ganglia in a rat model of neuropathic pain: Possible involvement in the development of neuropathic pain. Neurosci Res 2004, 48: 463–469.
28. Xie RG, Gao YJ, Park CK, Lu N, Luo C, Wang WT, *et al.* Spinal ccl2 promotes central sensitization, long-term potentiation, and inflammatory pain via ccr2: Further insights into molecular, synaptic, and cellular mechanisms. Neurosci Bull 2018, 34: 13–21.
29. Liu S, Gao H, Gao C, Liu W, Xing D. Bindarit attenuates pain and cancer-related inflammation by influencing myeloid cells in a model of bone cancer. Arch Immunol Ther Exp (Warsz) 2018, 66: 221–229.
30. Wu Z, Chang J, Ren W, Hu Z, Li B, Liu H. Bindarit reduces the incidence of acute aortic dissection complicated lung injury via modulating nf-kappab pathway. Exp Ther Med 2017, 14: 2613–2618.
31. Zhang ZJ, Jiang BC, Gao YJ. Chemokines in neuron-glial cell interaction and pathogenesis of neuropathic pain. Cell Mol Life Sci 2017, 74: 3275–3291.
32. McCoy ES, Taylor-Blake B, Zylka MJ. Cgrpalpha-expressing sensory neurons respond to stimuli that evoke sensations of pain and itch. PLoS One 2012, 7: e36355.
33. Han Q, Liu D, Convertino M, Wang Z, Jiang C, Kim YH, *et al.* Mirna-711 binds and activates trpa1 extracellularly to evoke acute and chronic pruritus. Neuron 2018, 99: 449–463 e446.